A Keynote Paper, Proc ACUN-4 "Composite Systems –
Macrocomposites, Microcomposites, Nanocomposites",
UNSW, SYDNEY, Australia, 21-25 July 2002
Eds : S. Bandyopadhyay et al, ISBN 0 7334 1862 7, pp. 61-72.

Recent Advancements in Manufacturing 3-D Braided Preforms and Composites[!]

Alexander Bogdanovich and Dmitri Mungalov
3TEX, Inc., 109 MacKenan Drive, Cary, North Carolina, 27511, U.S.A.
E-mail: bogdanovicha@3tex.com; Fax: 919-481-6595

Abstract

Several major directions of 3-D braiding technology and modern trends in the process and machine development are discussed. A novel 3-D step-wise rotary braiding process and automated machine are described next. Specific advantages provided by this 3-D braiding approach are discussed and illustrated by the fabricated items. Mechanical test data obtained for 3-D braided carbon fiber and E-glass fiber composites with different braid angle and content of axial fiber are presented and analyzed.

1. Introduction

Three-dimensional (3-D) woven and braided textile preforms for structural applications are gaining fast growing interest. A huge potential of 3-D woven and braided composites become more and more obvious with recent developments of automated, computer controlled machines capable of manipulating hundreds, even thousands of yarn ends in the 3-D weaving and 3-D braiding processes and thus satisfying the in-plane size and thickness requirements [1-5]. Importantly, while increasing the machine operation speed these technologies become competitive from the productivity viewpoint. It was well understood for a while that 3-D woven and braided preforms provide unique structural features and performance characteristics. Among those are full suppression of delamination, improved damage tolerance, impact resistance, better fatigue properties, higher strength near holes and openings, near bolts and fasteners, higher stiffener/skin attachment strength, etc. Besides that, using integral, seamless, near-net-shape thick fabric preforms eliminates from the manufacturing cycle a number of labor intensive operations like 2-D fabric ply cutting and stacking, tape slitting or prepregging, through thickness stitching, hand lay up with associated environmental issues, etc. Using RTM or VARTM processes with near-net-shape 3-D fabric preforms radically simplifies composites manufacturing and increases its cost effectiveness. This paper will address recent advancements in the area of 3-D braiding processes, machines and products. The readership interested in analogous aspects of 3-D weaving is directed to article [1].

Braiding is an ancient art, which can be defined, in modern terms, as a process of intertwining at least three parallel strands of fiber to fabricate continuous, seamless textile structure with non-orthogonal fiber orientation. Braiding is distinct from two other major textile processes, namely weaving and knitting, in the principal feature how the fiber strands are introduced into the fabric and placed there. In its advanced, automated computer controlled realizations, braiding processes provide highly flexible means of producing complex shape fabric preforms for composites at a rather high speed. At the same time, high precision of the desired fiber

architecture and the lateral dimensions of the fabric are achieved, thus enabling manufacturing near-net-shape or net-shape preforms. Three-dimensional braiding can be defined as the process where more than one "layer" of yarns are intertwined in the through thickness direction. However, using the term "layer" may not be adequate to the actual fiber architecture in many types of 3-D braided fabrics, because those do not have any visible features of common "layered" reinforcement. Nevertheless, historically the 3-D braiding processes were distinguished from conventional 2-D braiding by emphasizing that adjacent yarn "layers" are interconnected, thus an integral and comparatively thick fabric is produced.

A large bulk of literature is available on the subjects of braiding processes, machines and products, see for example publications [2-4,6-12]. However, in order to get familiar more intimately with technical details of 3-D braiding processes and their machine realizations, one needs to consult with the original patents, most of them issued in the last 20 years (a number of patents that have significantly influenced the progress and defined current status of 3-D braiding technology are listed in [5]). We concur with the authors of [9] that braiding in general and 3-D braiding in particular is not a simple science and engineering. The intimate knowledge of the processes and machines held by the industry experts is still important for a thorough understanding and successful application of this technology. On the other hand, it would not be right viewing braiding as just a collection of brilliant engineering solutions without substantial common grounds and close interrelation among them. As shown in a number of earlier publications ([3,6,9] are essential sources), numerous linkages can be found among diverse braiding processes and machines. In a recent publication [5] authors of this paper attempted a concise analysis of the roots, genesis and current state-of-the-art in some branches of 3-D braiding technology, focusing on the "rotary braiding" approaches. In order to clearly identify the place of a novel 3-D braiding process and machine (which is the major focus of this paper) a concise review of major directions of 3-D braiding technology is presented next.

2. Major Directions of 3-D Braiding Technology

Braided textile structures (ropes are the most common example) have been manufactured since the earliest civilizations. Thomas Walford is commonly credited as the inventor of the braiding machine on the basis of his 1748 patent for "an engine or machine for the laying or intermixing of threads, cords, or thongs of different kind." The next historic milestones are commonly credited to German inventor Bockmühl (1767) and French inventor Perrault (1784). The basic 3-D braid is fabricated by two orthogonal (horizontal and vertical) displacements of yarn carriers on a rectangular loom. 3-D braiding technology has advanced very rapidly since the patent [13] was issued for "Rapid Bias Weaving". The two major modern branches of 3-D braiding are: a "Cartesian" (or in its modified version cylindrical) braiding, also called "row and column" ("ring and column", respectively) and a "rotary" (also known as "horngear") braiding.

The Cartesian braiding allows individual control of each row and column's displacement and several steps in a braid cycle. A detailed analysis of different processes, devices and machines based on this approach can be found in [3]. As mentioned there, various types of 3-D braiding machines have been proposed by Bluck [13], Florentine [14], Weller [15], Brown [15], Popper [17], Spain and Bailey [18], and Brookstein [19]. The machines proposed in [13-18] belong to the category of through the thickness interlock, where each yarn travels from one surface of the fabric to the other and back. Contrary to that, the device [19] is an example of layer-to-layer interlock, where layer 1 is intertwined with layer 2, in its turn layer 2 with layer 3, etc., thus each yarn travels only within two adjacent layers. In any of the aforementioned through the thickness braiding approaches, fiber carrier travel is accomplished by, first, shifting columns in opposing directions, then shifting rows in opposing directions. Reversal of the direction of actuation in the second half of a shift cycle interlocks the fibers. Formation of a complex shape is possible by adjusting the number of positions shifted. Two most popular variants of this technological approach are termed "Four-step"

(examples are [13-16,18]) and "Two-step" [17] braiding.

When using Cartesian braiders, fabrication of various complex shapes is possible by adjusting the length of each row and column move (e.g., number of spaces shifted). Row motion is accomplished by shifting grooved tracks containing fiber carriers. Column motion consists of shifting the fiber carriers. Row and column motion can be mechanically or pneumatically actuated: the motion of an interior fiber carrier is caused by the push from an adjacent carrier, or by a shifting of the track beneath [20]. Since every fiber undergoes similar motion, all fibers become intertwined in a balanced array. Specific configurations of the fabric can be rectangular, semi-cylindrical, circular, or cylindrical. The first two geometries are used to produce rectangular or irregular shapes, while the circular and cylindrical braiders produce bodies of revolution. As pointed out in [3], there is an essential difference between making the two types of geometry: since the "body of revolution" machines are tightening the fibers around a mandrel, all fibers are under equal tension and the process is self-packing, while flat and irregular shapes have free edges where the fibers have different tension than in the center. A mechanical comb is then required to pack the braid tightly into the preform.

Probably, the most advanced, industrial scale automated 3-D braiding machine based on the patent [16] is comprehensively described in papers [3,20,21]. The machine was built by Atlantic Research Corporation and uses cylindrical braiding geometry. The machine is categorized as Through-The-Thickness Four-step, it holds 2880 fiber carriers distributed between 288 columns and 10 rings. It can produce diamond (1/1), regular (2/2) and triaxial ($0, \pm\theta$) braid patterns. Fiber angles can be varied from 30º (for preform width between 9 and 33 cm) to 70º (for width between 18 and 80 cm). The 10-ring machine construction can produce 0.5 cm thick fabrics for 80 cm width and 0.8 cm thick fabric for 11 cm width. Complex shapes can be fabricated on the ARC machine using so called "bifurcation patterns". As described in [3], this approach uses variable braid patterns to create unbraided regions or pockets within a preform. These regions are subsequently cut open and folded into the final configuration. In such a way the "bifurcation pattern" braiding, which is computer controlled, enables manufacturing relatively complex, integral structural preforms.

Along with many positive features of the "row and column braiding approach", a number of drawbacks and limitations are well known and have been discussed in the literature. One of them is that the yarn length on the carriers is quite small (for example, each fiber carrier of the aforementioned ARC braider has a capacity of 12 gram, which translates to approximately 30 m of 12K carbon tow). Also, the variety of fabric shapes and fiber architectures is limited; it is possible to fabricate the structures like I-, T-, box-beams, etc., however different machine bed configurations and specialized machines are required for different products. Another significant drawback is that there is no natural way to incorporate axial yarns in traditional Cartesian braiding process. This can be accomplished, particularly, on the ARC machine in a rather artificial way, by setting the machine operation pattern such as selected fiber carriers stay idle through the braiding cycle. When using this approach axial fibers are provided from the same carriers as the braid fibers. Thus, incorporating a relatively heavy axial tow in order to reach higher axial fiber content would ask stopping the machine for re-draw even more frequently. The alternative 3-D braiding approaches overcoming some of the aforementioned shortcomings and limitations of "row and column" braiding are considered next.

In the most popular, "classical" scheme of 2-D "circular braiding" (also called "tubular braiding"), there are two sets of yarns, which are intertwined, as illustrated in Fig. 1a. Importantly, all yarns are moved simultaneously: all yarns of one set are moved in the clockwise direction, while all yarns of the other set are moved in the counterclockwise direction. In 2-D circular braiding machine there are two intersecting tracks, one is traveled by those fiber carriers which move in clockwise direction and the other one by the fiber carriers moving in the counterclockwise direction. The fiber carriers are driven by continuously rotating horngears. The notches transfer the fiber carrier from one horngear to the other. The horngears must be positioned accurately at each intersection to provide smooth transfer.

When a fiber carrier reaches a track intersection, it is forced by the shape of the track to transfer to the next horngear. As pointed out in [9], specific realization of this transfer process is the heart of each particular braiding approach. The braiding machine where the fiber carriers are moved in the described manner is called a Maypole braider. It is pointed out in [3] that a conventional Maypole braider has certain disadvantages compared to the Cartesian-type machine. One of them is that the fiber carriers travel along sinusoidal paths that are longer than in the Cartesian-type machine; consequently, size of a Maypole braider is very large for a comparable number of fiber carriers. Also, the Maypole braiders are mechanically actuated, hence it is not possible to change braid patterns while the machine is running.

A continuous 2-D Maypole braiding approach gave birth to several invented mechanisms for 3-D continuous rotary braiding realization. The examples of a Cartesian construction can be found in [22,23] and cylindrical construction in [19,24]. In rotary 3-D braiding mechanisms some number of horngear units are assembled on a bedplate in certain configurations of rows and columns (usually square). One particular scheme of a square, 5x5 horngear arrangement is shown in Fig. 1b (this is similar to a broadly reproduced scheme of 4x4 horngear arrangement [7,8]); the respective braids were termed "diagonal" or "packing" braids in [7,8]. Various schemes of mechanisms aimed at transferring fiber carriers from one horngear to the other via special track construction were proposed in [22]. One particularly popular mechanism of this kind invented in [23] is illustrated in Fig. 1c. The mechanism works similarly to a railway switch. In order to change the braid cross-section or alternate the fiber carrier path, it is necessary to stop the machine and switch the track from the position that allows the carrier to be transferred to the adjacent horngear to the position that prohibits such transfer (or vice versa). A principal requirement to this scheme is that maximum number of occupied horngear wings (indicated by gray circles in Fig. 1) must be exactly the same as the number of empty ones (indicated by light circles). Accordingly, in the case of four horngear wings (illustrated in Figs. 1b and 1c) the maximum number of fiber carriers is twice less than total number of horngear wings. The described 3-D braiding approach can be realized in a continuous process and, consequently, the production speed would be relatively high when fabricating braids with constant cross section.

To the authors' understanding, some aspects of 3-D braiding approach [23], and particularly the track switch mechanism had been recently implemented in two 3-D braiding machines built by Herzog Braiding Machines company [25,26]. The first, prototype machine described in [25] has 10x10 horngear arrangement. In addition to the braid yarns the machine allows incorporating up to 181 axial yarns (100 of them passing via tubes through centers of all horngears and 81 through free spaces among each group of four horngears). According to [25], 50 axial yarns were used in T-stiffener braiding on this prototype machine. The second, most recent machine is a 9-module braider with 4x4 horngear arrangement in each module [26]. According to the requirement that only half of horngear wings can be occupied, the first of above braiders is limited to 200 braid yarn ends, while the second one to 288 braid yarn ends.

The transition of yarn carriers between adjacent horngears in the aforementioned rotary braiders is accomplished by the "switch point" mechanism, which can be either in "cycle" (transition prohibited) or "transfer" (transition allowed) position. Each horngear unit has its clutch-brake mechanism that allows it to either stop or rotate. All of the horngears and switch points are synchronized. As described in [25], the normally continuous braiding process is thus separated into a series of steps. During each step the switch points can be changed either to the "cycle" or "transfer" position, and the horngears can either rotate by 90º or stand idle. Keeping in mind that different fiber carriers cannot be moved to the same location in one step, an arbitrary movement of the carriers can be accomplished in such a step-wise process. This provides flexibility in producing variable cross-section braids.

Another popular 2-D textile technology, which is also based on a horngear rotation and transfer of fiber carriers, is 2-D "circular lace forming" illustrated in Fig. 2a. In contrast to 2-D "circular braiding" discussed above, the horngear rotation in this case is discontinuous. The process is a "step-wise". This textile process has also

originated a number of step-wise 3-D braiding processes and their machine realizations. One particular scheme is illustrated in Fig. 2b. The most important feature of this approach is that fiber carriers are transferred from one horngear to the other in discrete steps made by certain groups of horngears simultaneously. In order to design the braiding process in this case, it is first necessary to determine which horngears belong to each of the groups, considering that the trajectories of fiber carriers that have to be moved simultaneously (i.e., those belonging to the same group) could not intersect at the transfer points. Hence, in this process a motion of each fiber carrier is interconnected with the motions of many other fiber carriers, and designing kinematics of the braiding process is a complex task (one can use a popular puzzle to better understand the process).

Contrary to the scheme of Fig. 1b, in the scheme of Fig. 2b each horngear may hold not two, but four fiber carriers, though only one carrier is allowed take a "mutual" position between two adjacent horngears. Accordingly, the maximum number of fiber carriers is increased to 60 in the scheme of Fig. 2b compared to50 in the scheme of Fig. 1b. Still, 40 out of 100 horngear wings must be kept empty. At the same time, the process continuity and, hence, the production speed is substantially reduced. It should be added that braiding machines working on a step-wise horngear rotation principle use, as a rule, individual drives for each horngear in order to provide maximum flexibility to the process. However, this is not necessary – the process kinematics allows using common drives for certain groups of unrelated horngears.

Finally, a novel process of 3-D step-wise rotary braiding process has been recently invented at 3TEX, Inc. by the authors of this paper [29]. The braiding process inherits certain features of both 2-D circular braiding and 2-D circular lace forming processes. Schematic of this new process is illustrated in Fig. 2c. It is seen that in this particular scheme, all 100 horngear wings can be occupied by fiber carriers. Next section explains how this novel process can be realized in a 3-D braiding machine.

3. A Novel 3-D Rotary Braiding Machine

A novel type carrier switch mechanism invented in [29] is illustrated in Fig. 3 (the top view). In this scheme it becomes possible for two yarn carriers simultaneously taking place between adjacent horngears. The core elements of the machine include a horngear block with four horngear wings (Fig. 3a), a fiber carrier driver (Fig. 3b), and a rotary gripping fork (Fig. 3c). Generally, each horngear and each fork may use their individual drives. A connection of two horngears, rotating in opposite directions, via a rotary gripping fork is shown in Fig. 3d. As shown, there are eight fiber carrier drivers placed on eight horngear wings. Following this design, the machine can utilize maximum possible number of fiber carriers (all horngear wings are occupied) and, at the same time, provides maximum possible freedom of their transfer between the horngears. Indeed, any fiber carrier can be transferred, after certain number of steps, to any position on the bedplate by selectively activated rotary gripping forks. Important feature of the design is that the fiber carrier driver has two cylindrical surfaces, one with radius r of a horngear wing and the other with radius R of a rotary gripping fork. Using such transitional element, which serves as the holder for a fiber carrier, not only provides smooth transfer of the fiber carriers from one horngear to the other, but does it within minimal bedplate space (the yarn carriers are placed as close as possible to the center of a horngear). Thus the machine size relative to the given horngear wing size (which is determined in turn by the bobbin size) is minimized. One may recall that making a 3-D braider as compact as possible is highly important not only for producing larger braid cross-sections but also for compensating the yarn length change when the carrier moves from machine edge to the center.

The connection of two horngears via rotary gripping fork, shown in Fig. 3d, can be extended in both of the in-plane directions thus creating a machine module. Two square modules assembled from 16 horngears and 24 rotary gripping forks each are shown in Fig. 4. Note that the horngear assembly within a module can be arbitrary; the module configuration can be individually designed to mimic specific product cross-sections, for

example I-, T-, L-, J-, H-, Π, rectangular boxes, and other shapes of this type.

Further, an arbitrary number of modules can be assembled into a multi-module machine using the same rotary gripping fork mechanism. Analogously to the intra-module transfer of fiber carriers, a rotary gripping fork provides smooth transfer of the fiber carriers between adjacent horngears belonging to different modules. Again, the modules assemblage can be different, depending on the braid shape.

The described mechanical part of 3-D braiding machine has to be supplemented by a number of other systems. The drive system includes drive motors, gears, connectors, the common horngear drive for each module and individual drives for each gripping fork. In the current machine realization the drive system is pneumatic, although other types (hydraulic, electric, etc.) can be used if desired. The control system includes a computer processor, control software, acquisition sensors aimed at detecting positions of some moving machine components. In the current machine realization every module has its own independent control system, so the modules can be selectively activated or deactivated. As mentioned before, each intra-module and inter-module rotary gripping fork is activated individually. Finally, a very important part of the machine is a take-up system, which controls the braid angle.

Axial yarns are delivered from large bobbins placed outside the machine to the bedplate via tubes passing through the centers of all horngears. This means that for any desirable axial yarn size, its continuous supply can last longer than any continuous braid yarn supply. The prototype braider built with 16 horngears allows one using up to 64 braid yarns and 16 axial yarns. The second generation 9-module braider incorporating 144 horngears, enables using up to 576 braid yarns and 144 axial yarns.

A variety of 3-D braided fabric preforms can be manufactured on the described automated machines by simply changing the gripping fork activation pattern from the control computer, which normally takes several minutes. Axial yarns can be incorporated selectively, and their size at different locations can be varied, depending on the design requirements for specific composite products. For example, longitudinal modulus and flexural rigidity of a T-stiffener can be maximized for given structural component weight by distributing axial yarns nonuniformly across the web and flange areas. Generally, when designing structural components aimed at flexure loading, it is reasonable to incorporate more axial fiber near the outer surfaces.

Several product examples fabricated on the prototype machine are shown in Fig. 5. A continuously fabricated, variable cross-section carbon fiber braid starts as the solid square at one end and then changes to the I-beam, solid square again, then splits into two rectangles, those merge into the solid square again, which then changes to the T-section, solid square, hollow box, solid square, flattened cross-section, and ends up as the same solid square shape. It is necessary to point out that all horngears and all fiber carriers were employed when producing each of the above braid segments. This feature of the process and machine enables to maximize geometric parameters of each of the cross-sections while using fixed number of yarn ends. In the center of Fig. 5 there is carbon/epoxy integral T-stiffener braided on the prototype machine and consolidated in the mold. At the top of Fig. 5 there are 3-D braided E-glass strap and composite tensile member made by pultrusion.

One important aspect of the technology, which is only touched here, is computer modeling of the desired braid shape and fiber architecture (the latter one includes yarn size, braid angle and axial fiber content). Before producing some complex braided structure on the machine, it is necessary to exercise a model that relates the virtual fiber architecture (visualized in the predicted paths of all individual yarns within 3-D fabric) to the trajectories of fiber carriers that move on the machine bedplate and to the tension created by take-up mechanism. Two examples of such modeling are shown in Fig. 6: a square bar and T-stiffener, both characterized by some specific yarn size, braid angle and volume content of axial fiber. A simplified model, which does not exclude mutual yarn penetration, was used to generate the drawings.

4. Mechanical Characterization of 3-D Braided Composites

A variety of 3-D braided T300 carbon 12K yarn preforms were made on the prototype machine with different braid angles and different fiber content in axial direction. In all cases, 64 braid yarns and 16 strands of axial yarn were used. In the case of 50% axial fiber volume content, each axial strand contained four 12K yarns, while in the case of 20% axial fiber volume content, each axial strand contained one 12K yarn. All braided preforms were then consolidated in a closed mold using Abatron AboCast 50-3/AboCure 8012-7 epoxy resin. The mold with open edges was used in order to allow the excess of resin be released out of the work zone of test coupons. The mold pressure was applied via punch and was slowly increased to 1GPa during 30min. The processing temperature was 180F. Also, a control group of unidirectional coupons (further referred as 100% axial fiber) was made in the same mold by placing parallel 12K yarns.

Tensile and flexural tests were conducted at the Institute of Polymer Mechanics, Riga, Latvia under contract with 3TEX. All test coupons had rectangular cross-sections 8.6x6.9 mm. The tensile tests were performed in accordance with ASTM D3039/D3039M-95a, and 3-point flexure tests were performed according to ASTM D790-99. All coupons failed within the work zone or at the border between the work zone and end tabs. In the tensile tests the longitudinal strain ε_x and the transverse strain components, ε_y and ε_z, were monitored; two strain gauges bonded to the opposite surfaces of a coupon were used for each strain component. Then the data from each pair of strain gauges were averaged. Thus, the tests allowed obtaining three elastic characteristics: longitudinal elastic modulus E_x and two Poisson's ratios ν_{xy} and ν_{xz}. Also, the longitudinal tensile strength, σ_x^{tu}, and ultimate tensile failure strain, ε_x^{tu}, were obtained. The tests were performed at room temperature and relative humidity 60%. The loading rate was 1.5 mm/min. Test results are presented in Table 1. In the flexure tests the specimens had different length-to-thickness aspect ratios depending on the test plane. The tests were performed in two planes, *xy* and *xz*.. Two specimen lengths were used: 133mm and 70mm. Results presented in Table 1 characterize flexural modulus of the braided composites. The obtained results are compared to experimental data published earlier in [7].

It is worth noting that a very high (up to 71%) fiber volume fraction has been achieved in the fabricated composite specimens. The obtained V_f values are within the same range as in [7]. Also, the obtained densities of 3-D braided composites are very close to the data from [7]. It is seen from the test data comparison that Poisson's ratio values of the present 3-D braided composites are significantly lower that those reported in [7], and only for braid angles 23°, 36° and 42° they slightly exceed 0.5. The significant difference in Poisson's ratio allows to speculate that in spite of close total fiber volume fraction and braid angle values, there should be substantial difference in microstructure (including void content, possible microcracks within impregnated carbon yarns, debond and matrix cracks) of 3-D braided composites fabricated in this work and in [7]. The speculation is also supported by a huge difference in the tensile strength data to be discussed later.

Results in Table 1 for longitudinal elastic modulus obtained from the tensile tests are slightly higher than the respective results obtained from the flexure tests, with exception of two cases where the difference is within the scatter range. Also, the present tensile modulus results are considerably higher than the respective data from [7]. Further, the ratio of longitudinal modulus of 3-D braided composites to the control unidirectional composite changes from 0.47 (in the case of 0% axial fiber and 38.1° braid angle) to 0.96 (in the case of 50% axial fiber and 21° braid angle). The latter result indicates that incorporating substantial amount of axial fiber into 3-D braided preform allows to reach almost as high longitudinal modulus as for the respective unidirectional composite.

As seen in Table 1, the longitudinal tensile strength results for the present composites are dramatically higher than those reported in [7]. Particularly, in the case of 0% axial fiber and $\approx$20° braid angle the difference is 775MPa. It is

hard to explain such a huge difference for the materials made from the same fiber, resin, with similar total fiber volume fraction and braid angle. Besides possible differences in the experimental procedures, one guess may be that the composite microstructures were very different. Further, note that the strength ratio of 3-D braided to unidirectional composites, according to the present results, varies from 0.41 (in the case of 20% axial fiber and 36.4° braid angle) to 0.71 (in the case of 0% axial fiber and 19.3° braid angle). Thus, the longitudinal tensile strength reduction is more severe than the reduction of longitudinal tensile stiffness. However, it is understood that this inevitable loss of longitudinal strength is compensated by substantial improvement of other mechanical performance characteristics of 3-D braided composites. Experimental evidence of that can be found in [2,7,8,10,12] and other earlier publications.

Another mechanical characterization work was performed on 3-D braided/pultruded E-glass composites (see the top of Fig. 5). E-glass roving was braided in the form of rectangular straps and then pultruded with Atlac 580 resin. Rectangular, 16 x 4.5 mm cross section specimens were tested for tension and compression by Institute of Polymer Mechanics, Riga, Latvia. Test data are presented in Table 2 together with 3TEX results for 3-D woven E-glass "quasi-unidirectional" composites (in those 77% of all fiber was placed in the longitudinal direction) and the literature data for several unidirectional E-glass composites. The results presented here correspond to different resin systems, possibly also different E-glass rovings, and different composite processing techniques. However, certain conclusions can be made. Firstly, results for longitudinal modulus of 3-D braided composites in both 12˚ and 21˚ braid angle cases are in the range of other materials' characteristics. Secondly, longitudinal tensile strength of 3-D braided composites is considerably higher than for the 3-D woven composites but about 20% lower than for the unidirectional composites. Thirdly, compressive strength of 3-D braided composites is about twice lower than their tensile strength and seems to be the weakest property. From this one can make a recommendation that 3-D braided/pultruded E-glass composites may be used as predominantly tension-loaded structural components.

5. Conclusions

A novel 3-D rotary braiding process and its multi-modular, computer-controlled machine realization presented in the paper provides certain advantages over other 3-D rotary braiding approaches, particularly in minimizing the ratio of the machine bedplate size to the product cross-section size, and achieving the maximum flexibility in manufacturing complex, variable cross-section preforms.

Experimental 3-D braided Carbon fiber and E-glass fiber composites with different braid angle and different content of axial fibers were fabricated in the closed mold and also by pultrusion and tested for longitudinal elastic modules, Poisson's ratio, and longitudinal tensile and compressive strengths. Experimental results show that 3-D braided composites studied in this work have very good longitudinal elastic modulus and Poisson's ratio, excellent longitudinal tensile strength but quite poor longitudinal compressive strength. Additional mechanical characterization is needed to demonstrate performance advantages of 3-D braided composites to extend and diversify their industrial applications.

Authors' Resume

Dr. Alexander Bogdanovich, Vice President of Research & Development, 3TEX, Inc. Ph.D. from Institute of Polymer Mechanics, Riga, Latvia (1975), Dr. Sci. degree from Kazan' State University, Russia (1987), Dr. habil. sci. ing. degree from Latvian Academy of Sciences (1998). Two published books, over 130 journal articles and conference publications. Areas of expertise include Solid Mechanics, Mechanics of Composites, Computational Mechanics, Textiles and Textile Composites.

Dr. Dmitri Mungalov, Senior Product Development Engineer, 3TEX, Inc. Dr. sci. ing. degree from Latvian Academy of Sciences (1998). Over 40 journal articles, conference publications and patents. Areas of expertise include Textile Engineering, Textile Material Science, Mechanical Characterization of Composites, Biomechanics and Biocomposites.

References

1. M.H. Mohamed, A.E. Bogdanovich, L.C. Dickinson, J.N. Singletary, and R.B. Lienhart, "A New Generation of 3D Woven Fabric Preforms and Composites," SAMPE J., 2001, **37**, No. 3, pp. 8-17.
2. R.T. Brown, "Through-The-Thickness® Braided Composites for Aircraft Applications," The Ninth DoD/NASA/FAA Conf. On Fibrous Composites in Structural Design, November 4-7, 1991.
3. R.T. Brown and E.C. Crow, Jr., "Automatic Through-The-Thickness® Braiding," Proc. of the 37th Int. SAMPE Symposium and Exhibition, March 1992, Vol. 37, p. 832.
4. T.D. Kostar and T.-W. Chou, "Braided Structures," in 3-D Textile Reinforcements in Composite Materials, A. Miravete (ed.), Woodhead Publ. Ltd, Cambridge, England, 1999, pp. 21-240.
5. A. Bogdanovich and D. Mungalov, "Innovative 3-D Braiding Process and Automated Machine for Its Industrial Realization," Proc. 23rd Int. SAMPE Conf., Paris, April 9-11, 2002, pp. 529-540.
6. W.A. Douglass, Braiding and Braiding Machinery, Centrex Publishing Co., Eindhoven, 1964.
7. F.K. Ko, Engineered Materials Handbook, Vol. 1, Composites, ASM International, Metals Park, Ohio, 1987, p. 519.
8. F.K. Ko, Textile Structural Composites, T. W. Chou and F. K. Ko (eds.), Chapt. 5, Elsevier, Amsterdam, 1989, p. 129.
9. F.K. Ko, C.M. Pastore, and A.A. Head, Handbook on Industrial Braiding, Atkins & Pearce, Covington, Kentucky, 1989.
10. Tsu-Wei Chou, Microstructural Design of Fiber Composites, Cambridge University Press, Cambridge, 1992.
11. A.E. Bogdanovich and C.M Pastore, Mechanics of Textile and Laminated Composites, Chapman & Hall, London, 1996.
12. B. Cox and G. Flanagan, Handbook of Analytical Methods for Textile Composites, Version 1.0, Rockwell Science Center, Thousand Oaks, CA, 1996.
13. R.M. Bluck, U.S. Patent 3,426,804. February 11, 1969.
14. R.A. Florentine, U.S. Patent 4,312,261. January 26, 1982.
15. R. Weller, "AYPEX: A New Method of Composite Reinforcement Braiding," 3-D Composite Materials, NASA Conference Publication 2420, November 5-7, 1985.
16. R.T. Brown, U.S. Patent 4,753,150. June 28, 1988.
17. P. Popper and R. McDonnell, "A New 3-D Braid for Integrated Parts Manufacturing and Improved Delamination Resistance–The 2-Step Process," Proc. 32nd National SAMPE Symp., April 1987.
18. R. Spain and C. Bailey, U.S. Patent 4,984,502. January 15, 1991.
19. D. Brookstein, "On the Continuing Development of the Multilayer Interlock Braiding System," Fiber-Tex'91 Conference, Raleigh, NC, October 1992.
20. R.T. Brown and M.E. Harman, "Advanced Textile Braiding Techniques," America's Textiles International, Vol. 15, No. 7, July 1986, p. 74.
21. R.T. Brown, "Through-The-Thickness Braiding Technology," Proc. of the 30th National SAMPE Symposium and Exhibition, March 1985.
22. H. Reichel, U.S. Patent 3,894,470. July 15, 1975.
23. K. Bock and G. Flohr, U.S. Patent 4,096,781. June 27, 1978.
24. D. Brookstein, D. Rose, R. Dent, J. Dent, J. Skelton, U.S. Patent 5,501,133. March 26, 1996.
25. E. Laourine, M. Schneider, and B. Wulfhorst, Proc. of The 5th Int. Conf. On Textile Composites, Leuven, Belgium, 18-20 September, 2000.
26. Janpeter Horn, Managing Director, August Herzog Maschinenfabrik GmbH & Co. KG, Private Communication, JEC Composites Show, Paris, April 2002.
27. M. Tsuzuki, M. Kimhara, K. Fukuta, and A. Machii, U.S. Patent 5,067,525. November 26, 1991.
28. M. Tsuzuki, U.S. Patent 5,348,056. September 20, 1994.

29. D. Mungalov and A. Bogdanovich, Automated 3-D Braiding Machine and Method, U.S. Patent 6,439,096, August 27, 2002.
30. Composite Materials in Maritime Structures, Vol. 1, R.A. Shenoi and J.F. Wellicome (Eds.), Cambridge University Press, 1993.
31. I.M. Daniel and O. Ishai, Engineering Mechanics of Composite Materials, Oxford University Press, 1994.
32. Fiberite Materials Handbook, ICI Fiberite Technology Group, Tempe, Arizona, 1991.

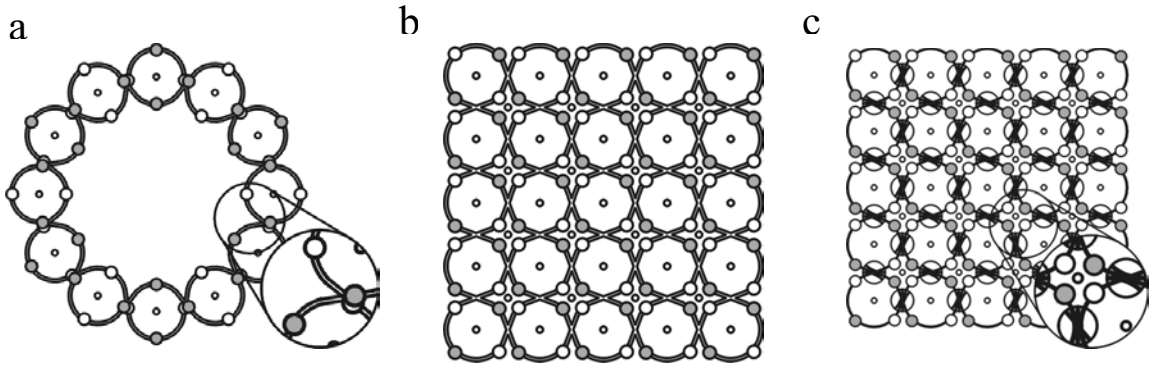

Figure 1. Schemes of 2-D Maypole braiding (a) and related prior art 3-D rotary braiding (b,c) approaches.

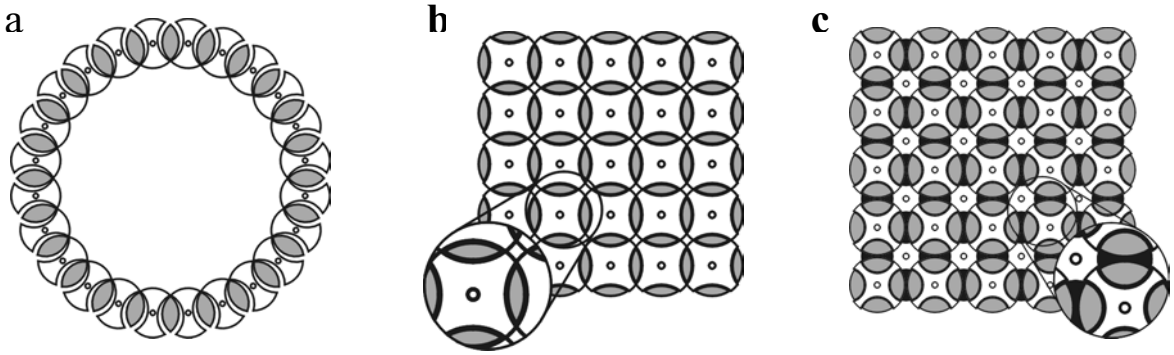

Figure 2. Schemes of 2-D Circular Lace forming (a) and related prior art (b) and 3TEX (c) 3-D rotary braiding approaches.

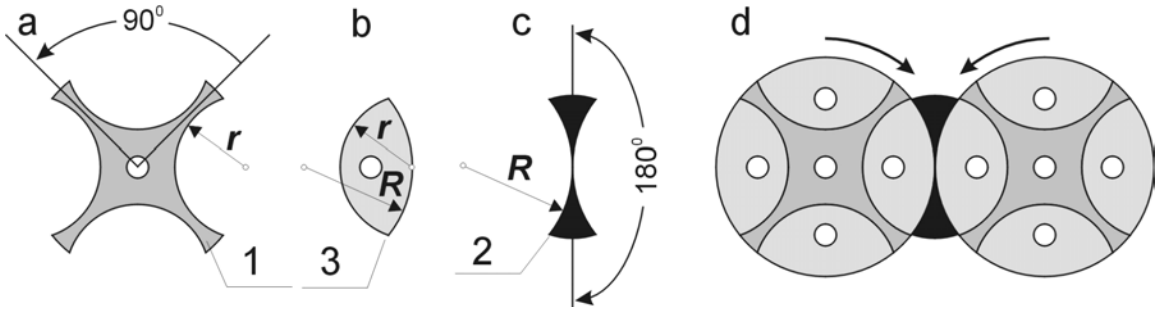

Figure 3. The yarn carrier switch mechanism invented for 3TEX braider [29].

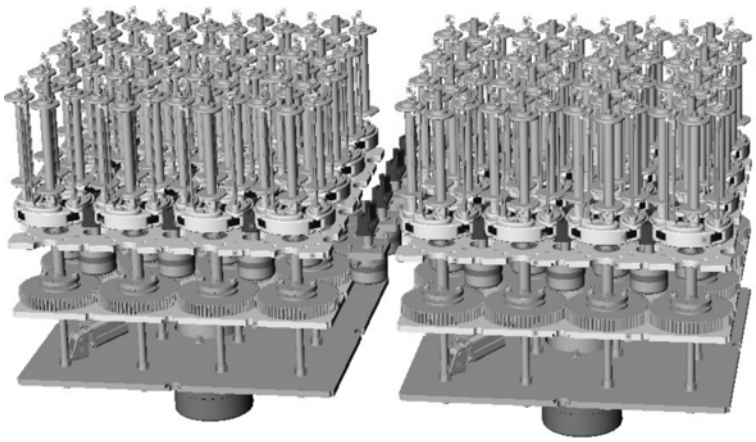

Figure 4. Two representative modules of 3TEX multi-module 3-D braider [29].

Figure 5. Continuously produced carbon fiber rope illustrating flexibility of 3TEX 3-D braiding process and machine. In the upper part: 3-D braided E-glass strap and pultruded composite.

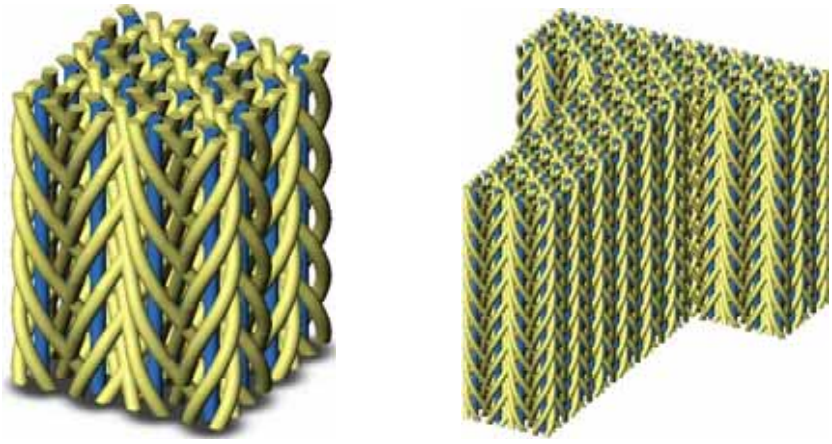

Figure 6. Design models of 3-D braided square bar and T-stiffener constructed from the yarn carrier movement patterns.

Table 1. Results of mechanical characterization of 3-D braided Carbon/Epoxy composites.

Tested material		Present results							Ref [7]		
Property		T300	T300	T300	T300	T300	T300	T300	T300 1 x 1	T300 3 x 1	T300 1 x 1
Percentage of axial fiber		0	0	20	20	50	50	100	-	-	50
Apparent fiber angle		38.1°	19.3°	38.9°	23.8°	42.3°	21.0°	0.0°	20°	12°	15°
Total V_f, %		67.6	71.0	64.1	64.0	66.6	71.3	67.4	68	68	68
Elastic modulus E_x, GPa	Tension	69.1	125.9	72.5	122.7	98.5	141.7	147.8	97.8	126.4	117.4
	Flexure	73.6	122.0	73.9	106.6	88.2	129.2	133.5	-	-	
Tensile strength, MPa		902.8	1441	827	1344	1024	1205	2026	665.6	970.5	790.6
Ultimate strain %		1.76	1.07	1.18	1.06	1.07	0.82	1.29			
Poisson's ratio ν_{xy}		0.716	0.486	0.553	0.564	0.507	0.370	0.277	0.875	0.566	0.986
Density, g/cm³		1.56	1.58	1.53	1.56	1.57	1.60	1.58	1.58	1.58	1.58

Table 2. Results of mechanical characterization of different E-glass composites.

Material Description	Fiber volume fraction in composite	Reference	Modulus of elasticity	Strength in tension	Strength in compression
	%		GPa	MPa	MPa
3BRAID™, pultruded E-glass/Atlac 580, braid angle 12°	52 total 10 axial	3TEX	42.1	843	413
3BRAID™, pultruded E-glass/Atlac 580, braid angle 21°	52 total 10 axial	3TEX	36.8	808	463
3WEAVE™, quasi-unidirectional E-glass/Atlac 580, RTM	63 total 49 axial	3TEX	39.0	750	790
3WEAVE™, quasi-unidirectional E-glass/Derakane 8084, RTM	53 total 41 axial	3TEX	46.0	500	440
Unidirectional, E-glass/Polyester	43	[30]	30.0	750	600
Unidirectional, E-glass/Epoxy	55	[31]	39.0	1080	620
Unidirectional, E-glass/948 Epoxy	55 - 60	[32]	41.0	1034	862
Unidirectional, E-glass/934 Epoxy	50 - 55	[32]	41-55	1034-1172	483-620